A Novel Technique for Measuring (Not Calculating) Young's Modulus, Poisson's Ratio and Fractures Downhole: A Bakken Case Study

Adam Haecker, James Lakings[2], Eric Marshall[2], Josh Ulla[2]
Fracture ID[2]

This paper was prepared for presentation at the SPWLA 58th Annual Logging Symposium held in Oklahoma City, Oklahoma, USA, June 17-21, 2017.

ABSTRACT

Rock mechanical properties such as Poisson's Ratio and Young's Modulus are essential to understanding well completions and predicting stimulation responses. Utilization of these in-situ measurements to design well completions has proven effective by allowing entry points to be placed within "like rock" groupings, yielding higher perforation efficiency during stimulation. However, the economic and operational burden to collect this data often prevents it from being collected regularly.

Current industry practice is to calculate these rock mechanical properties from dipole sonic logs. Unfortunately, the present level of technology for sonic tools yields measurement of, at most, three stiffness coefficients (C_{33}, C_{44}, C_{66}) in an ideal well. If the target formation is isotropic this is sufficient because only two coefficients are required to generate a fully realized solution. In a vertically transverse isotropic (VTI) formation, however, we must estimate the remaining unknowns including the critical C_{13} tensor (Quirein & Cheng, 2014 Modified ANNIE). Therefore, in order to fully describe the rock mechanics matrix, additional measurements or technology is required.

Continuous, high-resolution measurements of near-bit drilling induced vibrations provide an alternative technique to obtain these stiffness coefficients. Vibrations are recorded by mounting a set of tri-axial accelerometers on a 12" bit sub positioned directly behind the bit. In this recording configuration, the near-bit accelerations provide a measurement of the forces acting at the bit and the motions of the bit-rock interaction.

Typical values of near-bit accelerations used to represent the forces acting on the formation can be on the order of several gravities. Typical values of the displacement of the bit as determined from processing the near-bit accelerations are on the order of several micrometers. Because these values represent accelerations and displacements as opposed to stress and strain, geometric or other scalar corrections are applied to determine relative values of the mechanical rock properties. Thus, using these innovative new stress-strain relationships with respect to the material symmetry of formation and well orientation, it is possible to obtain the stiffness coefficients and thereby the rock mechanical properties.

There are, of course, potential issues with measuring rock mechanics while drilling; one is the question of whether the Young's Modulus and Poisson's Ratio are static or dynamic. The DDL data is more closely associated with the dynamic data since it is calibrated to the dipole sonic tool response. Therefore, static to dynamic corrections are still required. Also, changes in downhole assemblies and drilling techniques must be accounted for in the processing.

A comparison from a two-mile lateral in the isotropic Bakken reservoir near Williston, ND, is presented contrasting open-hole horizontal logs including triple combo, dipole sonic, image logs and this new downhole rock mechanics measurement. Post-processed data shows rock mechanical properties can be positively identified using this new technology.

INTRODUCTION

Drilling long length horizontal wells in unconventional reservoirs has provided operators an unprecedented opportunity to characterize lateral heterogeneity of reservoir rock properties, in ways far superior to the sparse vertical sampling previously afforded by conventional well logging programs.

Unfortunately, the interest in the lateral variability of rock properties is often masked in practice by geometrical wellbore completion designs where specified stage lengths and perforation intervals often outweigh, or are commonly believed to overcome

A

any considerations regarding the natural, in-situ state of mechanical rock properties or geological variability along the length of the wellbore.

This issue becomes further exacerbated by the nature of conventional well logging programs and other borehole measurements that were originally conceived and largely designed to measure rock properties which for the most part were taken only to vary vertically stratigraphically and may not be well suited for unconventional, horizontal logging environments.

This has led to approaches for reservoir characterization that emphasize model completions strategies where lateral variations in mechanical rock properties are taken to be mainly continuous and isotropic, such that any lateral variability in mechanical rock property and the mechanical rock property relationships along the length of a wellbore are subsequently understood to be occurring in relation to the trajectory of the geo-steered well with respect to linear extrapolations of the structural dip of the vertical, mechanical stratigraphy.

In exploration and exploitation of unconventional resources, the forecast of the various formation lithologies and properties are usually maintained as constant along the length of a wellbore. Sometimes, it is even considered to be constant over several contiguous pads or sections throughout the reservoir in question.

However, when drilling in and through complex reservoirs where the lateral variability in rock properties and rock property relationships with respect to the underlying formation are expected to be strong and occur over inter-well lengths, then the assumptions implied in the application and use of geometrical staging designs to initiate, propagate and maintain hydraulic fracture permeability may fall short of long-term expectations for production and incremental reserve adds.

This is unfortunate, because mechanical rock properties and rock property relationships have been found both in the laboratory and in-situ to naturally arise out of the way the drillbit interacts with a rock.

By characterizing the way a rock formation drills may be useful to describe how the rock formation will fracture or break when undergoing hydraulic fracture stimulation treatments.

This paper will describe an innovative new technique involving the processing and analysis of drilling induced vibrations to obtain mechanical rock properties and rock property relationships. These relationships are evidenced against dipole sonic measurements. Finally, a completion design that responds to the mechanical rock property heterogeneity is introduced with a view towards improving perforation efficiency.

METHODS AND TECHNIQUES

Background: High-rate laboratory measurements of drilling induced vibrations indicate that the broad-band spectral power of the acceleration spectra from a PDC bit can be viewed in terms of a continuum of discrete elastic dislocations or acoustic emissions (Nakken et al, 1990). In other words we can view the PDC bit action as sound waves.

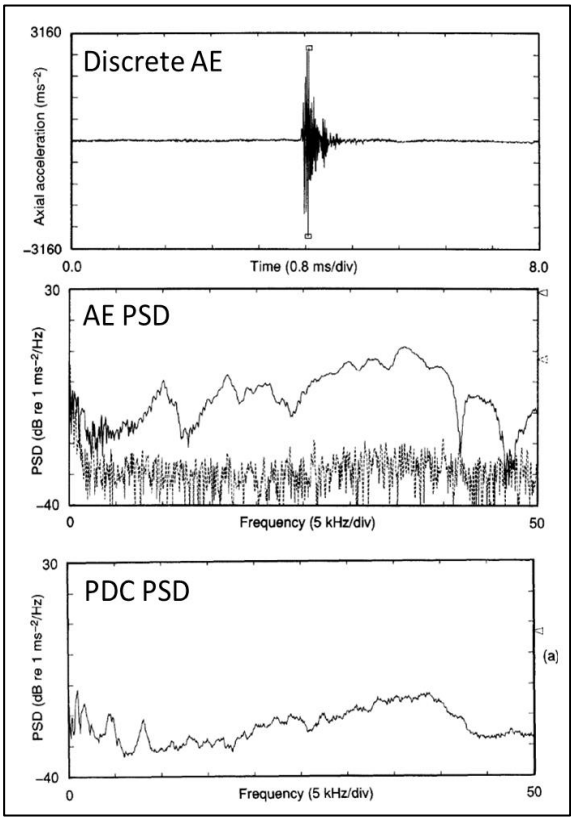

Figure 1. Modified from Nakken et. al., 1990. Hi-rate, laboratory measurements of drilling induced vibrations show that the power spectral density (PSD) spectra of a PDC bit is like that observed for a discrete acoustical emission (AE) event.

Other later laboratory investigations have, (a) further elaborated on the application and use of statistical moments to analyze drilling acceleration spectra, (b) used these data to populate non-linear regression models to classify rock lithologies, and (c) demonstrated that statistical descriptions of the acceleration spectra are in fact the dominant components needed for obtaining a successful lithological classification (Esmaeili et al., 2013).

Additionally, the acoustic energy or sound generated by drilling noise have also been found to correlate well to mechanical rock properties (Kumar et al., 2011).

These observations strongly suggest that the spectral characteristics of a drill bit interacting with a rock formation may, in fact, be dominated by geology.

Because it is difficult to replicate in-situ drilling conditions in laboratory investigations, it is often unwieldy to meaningfully extrapolate these types of spectral classification schemes or regression estimates of rock properties into the field.

Given that, (i) the spectral character of the drilling induced vibrations is shaped by a continuum of dislocation pulses or acoustic emissions, and (ii) statistical descriptions of the spectral shape are found to correlate with rock lithology, this naturally lends itself to an approach that involves well-understood geophysical signal processing techniques commonly used by earthquake seismologists to parameterize microearthquake source mechanisms (Brune, 1970).

That is, it is believed that the geometry of the bit interacting with a rock formation behaves in a manner similar to the mechanics of faulting, where the radiation of elastic waves from the rubbing together of two rugose, corrugated surfaces appears like band-limited Gaussian noise, and can be processed using the Brune parametric spectral representation of the seismic source to determine the displacements and stress drops acting across those surfaces.

The application and use of parametric representations of micro-earthquake source mechanisms are used to characterize continuous, high-frequency, tri-axial drilling induced vibrations. The mechanical rock properties from this method are compared to those obtained from traditional wireline sonic measurements to design a completion program.

Data Acquisition: Continuous, high-resolution measurements of drilling induced vibrations were taken using a downhole data logger (DDL or the "tool") consisting of a tri-axial accelerometer package set to sample at 1 kHz placed in both a near-bit and string-sub recording positions.

This tool operates in memory mode only. Other than on-board low-pass antialiasing filters, all data processing is done after the data has been downloaded from the tool.

The tri-axial accelerometers are mounted on the subs such that the centripetal axis of the accelerometer is perpendicular to the drill collar and the two lateral channels record motions in the plane tangential to the drill collar. The orientations of the channels tangential to the collar are generally unknown owing to the way the tool is screwed into the sub about the axis of the centripetal or radial accelerometer channel until the specified torque is achieved.

In some instances, the tool may be shimmed to align the accelerometers parallel to the face of the drill collar such that one is oriented in the axial direction and the other is oriented in the tangential direction. Barring this, the orientation of the accelerometers can be obtained directly afterwards by using the gyro to rotate the accelerometer pairs.

The initial processing applies a series of digital filters to remove onboard electronic noise.

Figure 2. Side view of bit sub. DDL recorder is puck shown in center of sub. Length of sub is approximately 12". Centripetal or radial channel is pointing out from page.

Data Processing: The acceleration data are processed in the frequency domain where they are integrated to obtain displacement spectra. The Fourier transforms decompose the frequency components of the acceleration of the bit over sample windows specified in powers of two. When drilling at 120 RPM, a 512-sample window would correspond to one turn of the bit. So for example, drilling at 240 RPM would imply a rotational frequency of four hertz and at the native sample rate of 1 kHz would involve approximately 256 samples per turn of the bit

Bandpass filters are applied to remove lower frequency noise in the data that is typically understood to be to be related to drilling string and BHA harmonics.

Bandlimited estimates of the root-mean-square (RMS) accelerations and zero-frequency level (ZFL) of the displacement spectra over these window lengths are then obtained. The displacements measured by these methods are typically on the order of a micrometers and the RMS accelerations are on the order of a few gravities. Because only a single tri-axial accelerometer is used in the processing, the ZFL of the displacement spectra and the RMS estimates of the accelerations can contain both angular and linear motions.

Comparisons of the processed acceleration data are found to compare well with downhole measurements of above-motor torque on bit and weight on bit. High-frequency, downhole measurements of near-bit torque and weight are presently unknown or unavailable for comparison with respect to the method here, only that it is believed that the near-bit acceleration should provide a better approximation for the stresses at the bit than what is measured above motor. This understanding is consistent with laboratory measurements that show a strong correlation between the acoustical emissions and torque applied (Karakus et al., 2013).

As an aside, it is interesting to note that historically, most processing of drilling induced vibrations generally involved focusing on the lower-frequency components that carried the increased levels of shock and vibration energy that was would be most damaging to the BHA. Overlooking the higher-frequencies may have obviated the understanding of using drilling induced vibrations to undertake formation evaluation using these data.

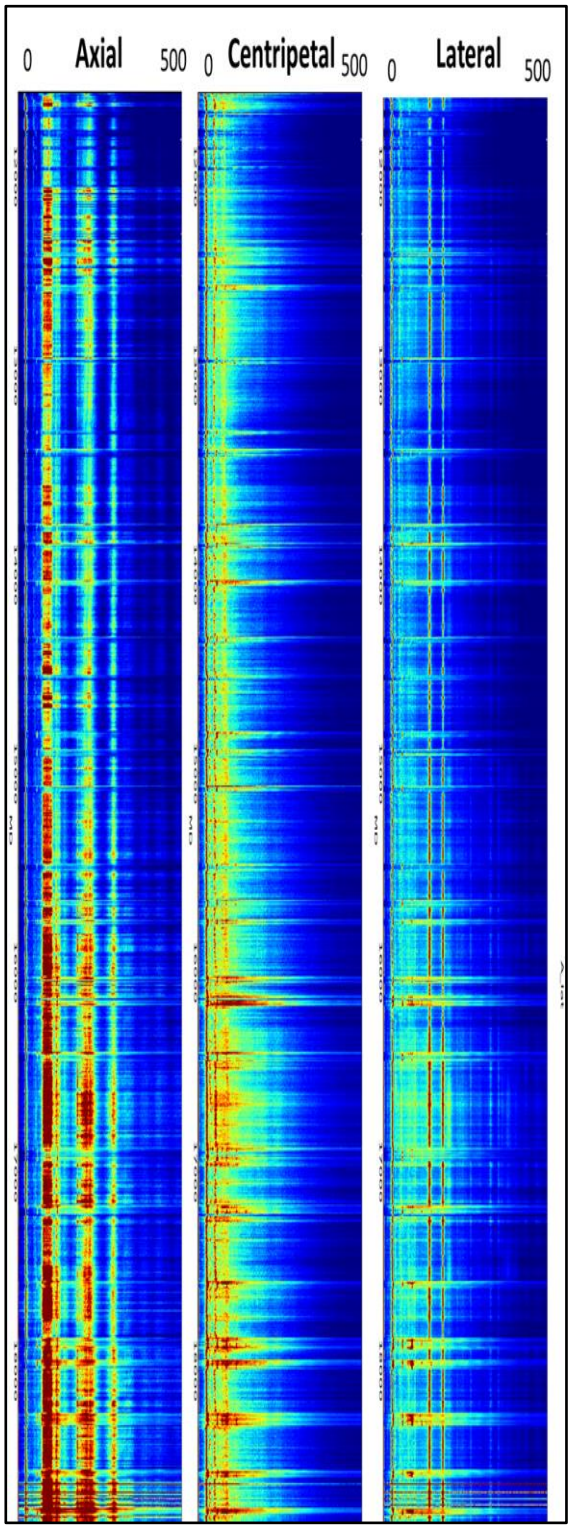

Figure 3. Acceleration spectra by depth for Run 1 of the lateral. Only data while drilling is shown.

A

Stress and Strain: Because the processed data are expressed in terms of forces and displacement, they must be converted into stresses and strains to obtain mechanical rock properties. One of the ways to accomplish this is to normalize the forces by the area of the bit and normalize or scale the displacements by some characteristic or reference length such as a depth of cut or the cutter diameter to obtain a strain. However, because the cutting structures of the bit are complex and the effective contact areas for the weight and torque are expected to be markedly different, simple geometrical scaling of the input data is unlikely to provide realistic values of mechanical rock properties.

We use an innovative, new method to obtain a set of coefficients or scalars (A, B, C, D, E, F) through the processing and analysis of drilling induced vibrations measured while drilling a material or rock formation with known mechanical properties that are understood to, (i) account for the geometrical considerations and other factors such as the radiation and transmission of elastic waves at the bit-rock interface, and (ii) transform the MWD data into the stress and strain that is experienced by a material or rock formation interacting with a drill bit as follows:

Matrix A

$$\begin{bmatrix} -a_1 & 0 & 0 & d_1\overline{C_{11}} & d_2\overline{C_{12}} & d_3\overline{C_{12}} \\ 0 & -a_2 & 0 & d_1\overline{C_{12}} & d_2\overline{C_{11}} & d_3\overline{C_{12}} \\ 0 & 0 & -a_3 & d_1\overline{C_{12}} & d_2\overline{C_{12}} & d_3\overline{C_{11}} \end{bmatrix} \begin{bmatrix} A \\ B \\ C \\ D \\ E \\ F \end{bmatrix} = \begin{bmatrix} 0 \\ 0 \\ 0 \end{bmatrix}$$

This stress-strain relationship represents a homogeneous system of linear equations that can be solved for the scalars from measurements taken while drilling an isotropic material where the mechanical properties are previously known, such as, for example a cement. Here the displacements or "d" terms and the accelerations or "a", terms are specified respectively in terms of, (i) the axial, angular, centripetal and/or lateral displacement of the drill bit, and (ii) the axial, angular, centripetal and/or lateral accelerations of the bit.

It would also be possible to represent the "a" terms using MWD of the weight on bit and the torque on bit where the solution to the scalars would represent the effective contact areas of the bit with respect to the orientation of the forces being applied to the bit.

The reference set of elastic properties, here referred to as the isotropic stiffness coefficients, C_{11} and C_{12}, can usually be obtained by offset sonic measurements or from processing the MWD data when drilling a material or rock formation in the well with known mechanical rock properties such as a cement. For the processing employed here the initial elastic properties were a Young's modulus of 7.73 Mpsi and a Poisson's ratio of 0.25.

The solution to the system of equations provides a single set of scalars that is applied to the input data for the length of the lateral.

The use of a single set of scalars to process the MWD data can be thought of like this: if the rock properties along the length of the lateral are constant and isotropic, and the drilling conditions vary, which they will, then the variations in the stress and strain caused by the variations in the applied drilling parameters would still fall along a locus of points that defines or otherwise describes the elastic portion of the stress-strain curve of that particular Young's modulus and Poisson's ratio elastic coefficients.

The MWD data consisting of the forces or accelerations, and displacements are transformed to a corresponding stress and stain with respect to the corresponding scalar value. The isotropic stiffness coefficients can be obtained by processing the scaled MWD data using stress-strain relationships. Again, these are only informed using a single set of scalars along the entire length of the lateral as follows:

A

Matrix B

$$\begin{bmatrix} Dd_1 & (Ed_2 + Fd_3) \\ Ed_2 & (Dd_1 + Fd_3) \\ Fd_3 & (Dd_1 + Ed_2) \end{bmatrix} \begin{bmatrix} C_{11} \\ C_{12} \end{bmatrix} = \begin{bmatrix} Aa_1 \\ Ba_2 \\ Ca_3 \end{bmatrix}$$

Anisotropic Stiffness Coefficients: Although the rock in this Bakken formation is expected to be isotropic, one of the concerns in this play is the possible influence fractures on the production of this reservoir. Because variations in the isotropic stiffness coefficients are probably inadequate to describe the influence of fractures on the rock properties, it is worthwhile to explore the possibility of fracture induced anisotropy by solving for a transversely isotropic (TI) representation of the media to infer the nature and occurrence of pre-existing fractures along the length of the lateral.

The methodology used to obtain the isotropic stiffness is extended to the TI case. Here, the MWD data are processed using a TI stress-strain relationship to obtain the anisotropic stiffness coefficients as follows.

Matrix C

$$\begin{bmatrix} Dd_1 & Ed_2 & Fd_3 & 0 \\ Ed_2 & Dd_1 & Fd_3 & 0 \\ 0 & 0 & (Dd_1 + Ed_2) & Fd_3 \end{bmatrix} \begin{bmatrix} C_{11} \\ C_{12} \\ C_{13} \\ C_{33} \end{bmatrix} = \begin{bmatrix} Aa_1 \\ Ba_2 \\ Ca_3 \end{bmatrix}$$

Note that when solving for the TI stiffness coefficients it is important to account for the orientation of the drilling well with respect to the orientation of material symmetry. For example, a laterally drilling well in vertically transverse isotropic (VTI) media, the d_1 and a_1 terms would respectively represent the axial displacement and axial acceleration.

In practice because there are only three equations and four unknowns the solution is constrained by making an approximation where C_{12}=C_{13}. This approximation is not without precedent and may provide a logical first step to introduce more empirical relationships when available to advance anisotropic descriptions (Murphy et. al.,, 2015 Modified ANNIE).

Note that the same scalars used to obtain the isotropic stiffness coefficients are also used to obtain the TI stiffness coefficients.

The technique could be extended to include the possibility of scaling the input data to known or a-priori values of the anisotropic stiffness coefficients, but these can be highly variable and difficult to obtain, therefore the state of the art is to use the scaled inputs referenced to the isotropic solution to solve for the anisotropic stiffness coefficients.

Fracture Identification: The fracture identification technique looks for systematic variations in the elastic coefficients parallel to bedding and perpendicular to bedding. For most VTI media, the rock appears more compliant when loading perpendicular to bedding than parallel to bedding. This introduces a construct such that when the vertical Young's modulus is greater than the horizontal Young's modulus this would indicate that the rock is more compliant in a horizontal direction then in a vertical direction. This "cross-over" or reversal in the expected relationship between the horizontal Young's modulus and the vertical Young's modulus contrasts what would normally be expected for a VTI representation of the stiffness coefficients.

By identifying instances when the horizontal Young' modulus is less than the vertical Young's modulus the rock would be considered fractured. Likewise, if there is a strong increase in the horizontal Young' modulus relative to the vertical Young's modulus, then the rock would be considered laminated or strongly bedded. For isotropic rock, the differences between the horizontal and vertical Young's modulus would be small or near zero. Therefore any deviations from zero indicate the probable presence of fractures.

Because it is typically observed that the absolute values for the anisotropic stiffness coefficients obtained under the current construct are systematically offset or biased from one another, the method compares the differences between mean-subtracted and variance normalized representations of the vertical and horizontal Young's modulus terms (eqn. 1)

$$\frac{E_h - \overline{E_h}}{\sigma} < \frac{E_v - \overline{E_v}}{\sigma} \quad (1)$$

The presence of fractures are viewed in terms of the relative behavior of the anisotropic Young's modulus curves. The comparisons between the horizontal and vertical Young's modulus are taken after a mean subtraction of the curves and therefore only represent relative values and are difficult to quantify further. Additionally the anisotropic Young's modulus terms require the aforementioned estimation of C_{13} based on C_{12} which further compounds the relative nature.

Future constructs that involve effective media theory that use fracture compliances to identify fractures may be more appropriate because, (i) it is possible to compare the variations in anisotropic media against a background isotropic model, (ii) the differences between the effective and background media can be expressed in terms of single stiffness coefficients instead of the elastic coefficients, and (iii) the differences can be expressed terms of the actual values of the stiffness coefficients as opposed to using a mean subtract to do so.

CASE STUDY RESULTS

Location and Data Collection: The Devonian Three Forks (TF) formation is located in the western two thirds of North Dakota in the Williston Basin province. (Fig. 5) It lies below the Bakken formation and above the Birdbear Formation. (Fig. 6) The Three forks formation is sourced from the prolific organic shales in the Bakken Formation. The well that is the focus of this case study was located in Dunn County, North Dakota and targeted in the 2nd bench of the Three Forks. The study well was drilled horizontally for 10,400' once the target depth was achieved.

Open-hole logs including a gamma ray, induction resistivity, density porosity, neutron porosity, and a dipole sonic tool were measured on both a nearby vertical well and the subject horizontal TF well. Further, in the horizontal well, an image log was acquired to compare the fracture flag from the DDL tool to image log picked fractures. Additionally an adjacent vertical well had core retrieved and static rock mechanics measurements were made on plugs in a triaxial load frame. Finally, as is the purpose of this paper, a downhole data logger (DDL) consisting of a tri-axial accelerometer package set to sample at 1 kHz was inserted approximately 50' behind the bit to measure elastic properties via the techniques presented in the previous methods section. All of these data sets were compared to determine the accuracy of the DDL tool.

The DDL tool failed during part of one run and thus there is a ~2000' gap in the data located about 75% down the length of the lateral.

In the heel of the well, the dipole lost coherency and this resulted in spurious results in the sonic calculated mechanical properties.

Well Steering: The case study well was targeted in the second bench of the Three Forks Formation between two shale intervals known within the company as Internal Shale 1 and Internal Shale 2. (Fig. 4) The well immediately exited the target zone upon landing in the TF formation. From there it slowly climbed back into the bottom of the target zone before exiting out the bottom again approximately halfway-down the length of the lateral. The well then returned to the target formation and alternated from the top to the bottom of the target window for the remainder of the lateral.

This was beneficial from a data collection standpoint as it allowed us to see the majority of the reservoir interval even in a horizontal well. It seems so often that horizontal well logs just show the same values for the entire length of the well. Also it provides an opportunity to test the response of the DDL tool in a variety of different mechanical benches and contrast the data with the dipole acoustic log.

A

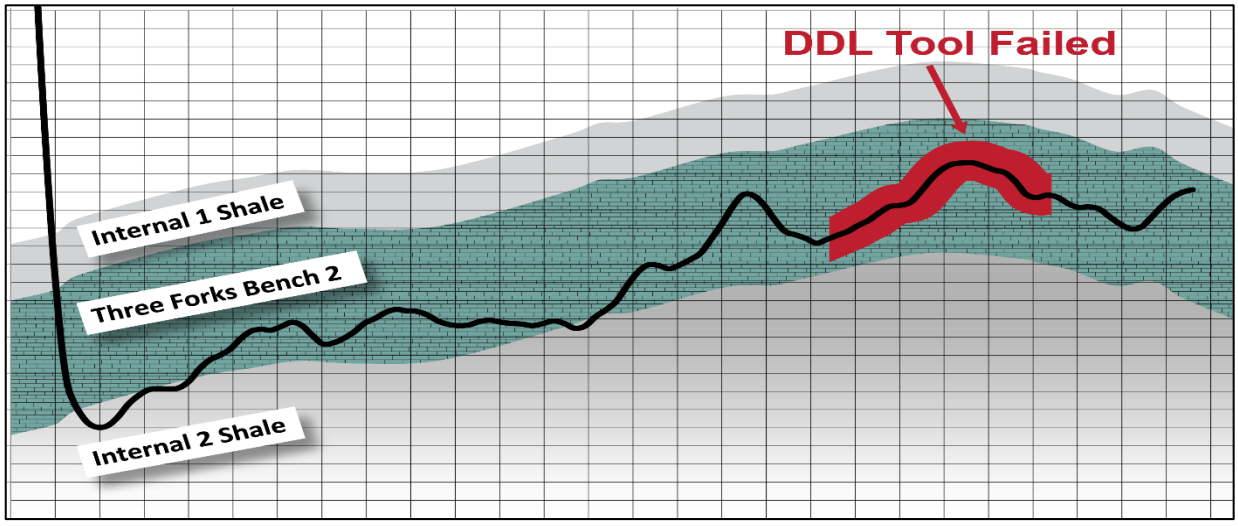

Figure 4. Diagram of the well trajectory through the Three Forks 2. Note the tortuosity of the wellbore and tool failure near the toe of the well.

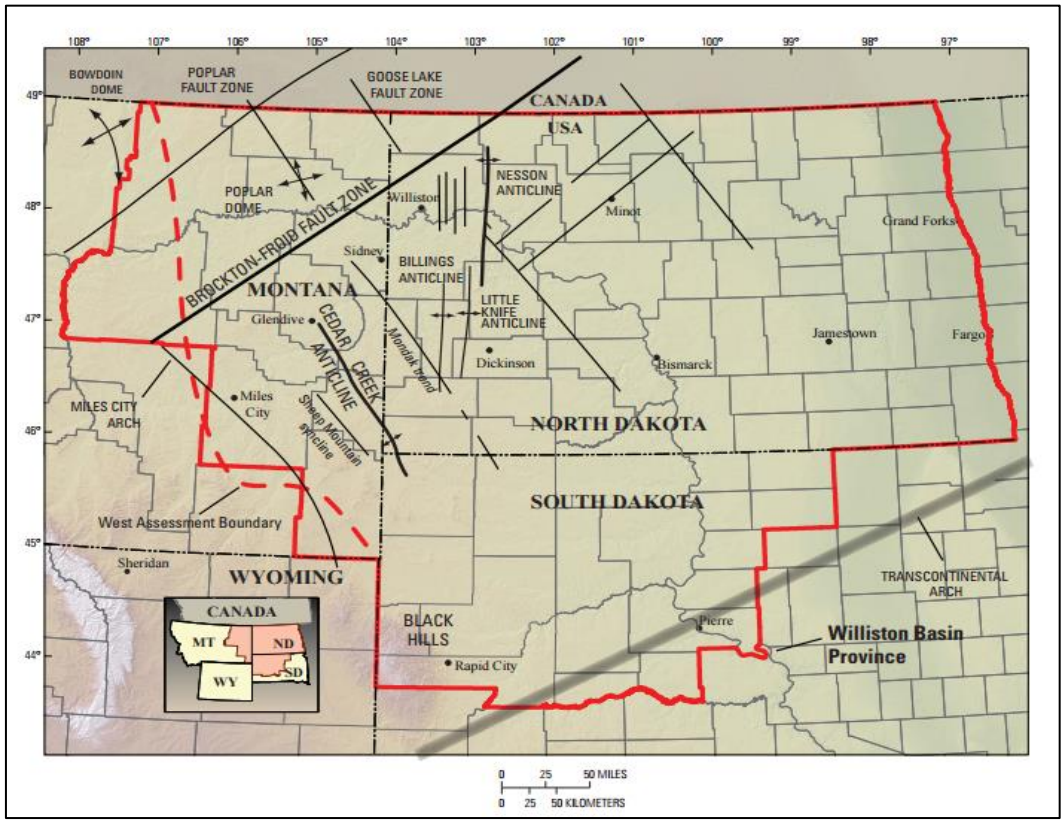

Figure 5. Map of the Williston Basin with prominent geologic features.
Source: US Geological Survey Williston Basin Stratigraphic Framework. L.O. Anna et Al., 2013

A

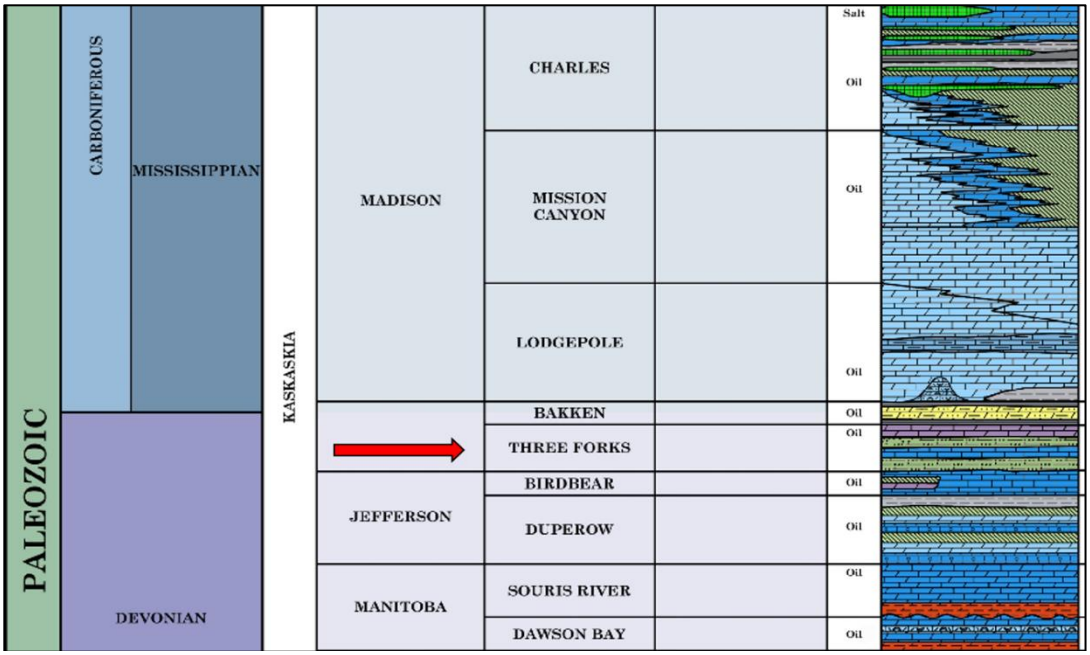

Figure 6. Shortened strat column of the Williston Basin, highlighting Three Forks formation.
Source: North Dakota Stratigraphic Column, ND Geological Survey, Murphy, E.C.et. al., 2009

Tensors: The Three Forks formation has been empirically shown to be linear elastic and isotropic based on both lab tests and horizontal well data compared to vertical well data. Therefore it uses the isotropic elastic stiffness matrix (Appendix A) and requires just the compressional velocity, shear velocity and bulk density to fully characterize its' elastic properties. The comparison of the calculated tensors from dipole (red) are compared to the calculated tensors from the DDL (black) tool (Fig. 8). The data is displayed in gigapascals.

Given that the DDL tool is recording the three different accelerations and converting to tensors via matrix B

$$\begin{bmatrix} Dd_1 & (Ed_2 + Fd_3) \\ Ed_2 & (Dd_1 + Fd_3) \\ Fd_3 & (Dd_1 + Ed_2) \end{bmatrix} \begin{bmatrix} C_{11} \\ C_{12} \end{bmatrix} = \begin{bmatrix} Aa_1 \\ Ba_2 \\ Ca_3 \end{bmatrix}$$

The C_{11} and C_{12} are being directly calculated from the accelerations while the C_{44} tensor is being calculated due to symmetry (Appendix A). The results show good matches between C_{11} from the DDL and the dipole C_{11} with the exception of near the heel of the well. The dipole lost some coherency in both the shear and compressional due to well bore conditions and bed inclination at the heel of the lateral.

It should be noted that all of the tensors in the formation have a relatively small dynamic range. C_{11} is slightly log-normal with a P50 of 70 GPA and a standard deviation of 2.76 GPA. C_{12} is very normally distributed around 25 GPA with a standard deviation of 2.57 GPA. Finally, C_{44} is normally distributed around 22 GPA with a standard deviation of 1.53 GPA and it has the smallest range. (Fig. 7) The low dynamic range is likely due to the homogeneity of the Three Forks formation in the Williston Basin. Changes seen in the tensors are due in part to how tortuous the wellbore was and how much section was cut during the drilling process. (Fig. 4)

Additionally, it is interesting how much the Sonic C_{44} tracks the DDL C_{44} considering that we are not even solving for it in matrix B. The C_{12} arguably has the worst match between the three tensors. However if we were to speculate it is possible that the C_{12} value is acting as a coupling term for some bit action that is actually a function of the C_{44}. This is an area for further research.

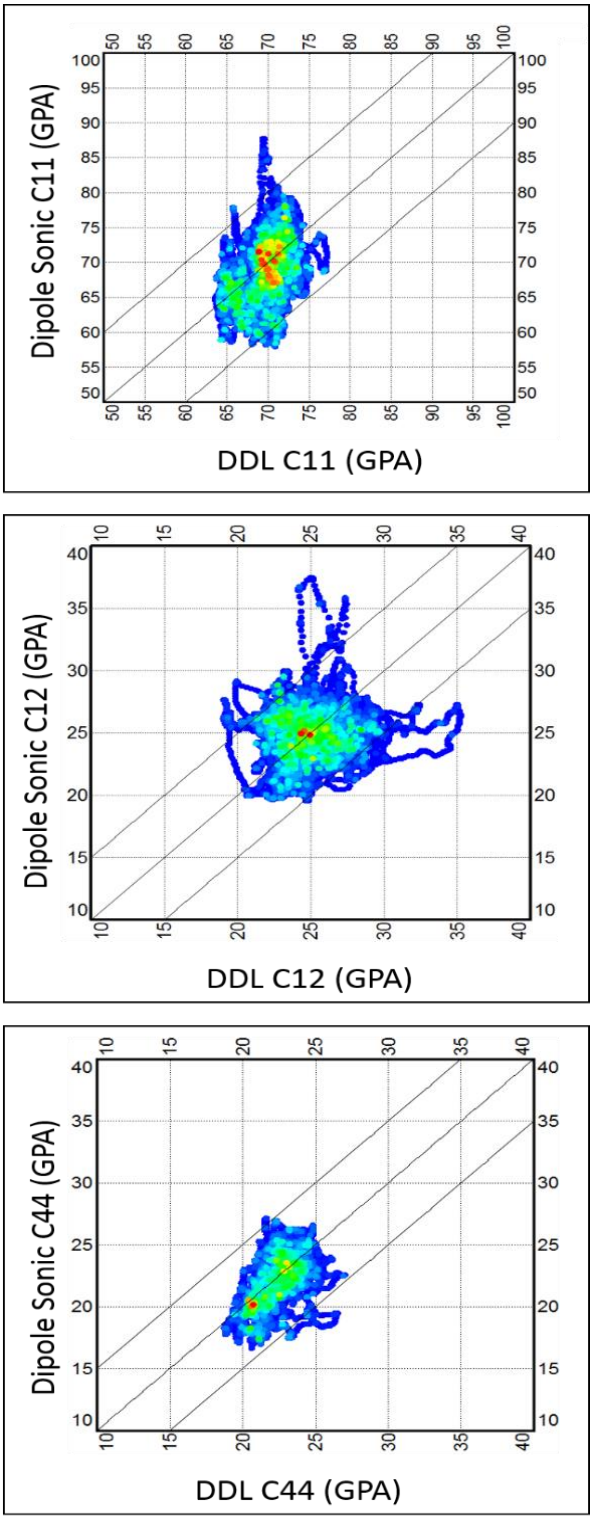

Figure 7. Cross plots of the tensors extrapolated from the DDL data, and the wireline dipole derived tensors. The plots have 1-1 lines with +/- 5 or +/-10 GPA lines

A

It is beneficial to have an offset dipole log with this technology so you can refine the constants A-F from matrix B. Until more rigorous lab tests are complete, this a-priori knowledge will be essential to constraining the solution. Luckily most basins in the world have a few dipole sonic logs available for comparison. Conceivably after a sufficient number of jobs in a given basin convergence of constants would be found for different formations and drilling environments but currently, there is not sufficient data to predict the values of A-F in any given environment making a dipole necessary to constrain the relative nature of these relationships. In summation, it is necessary to have *some* bit of information to properly constrain matrix B in order for this new method to work.

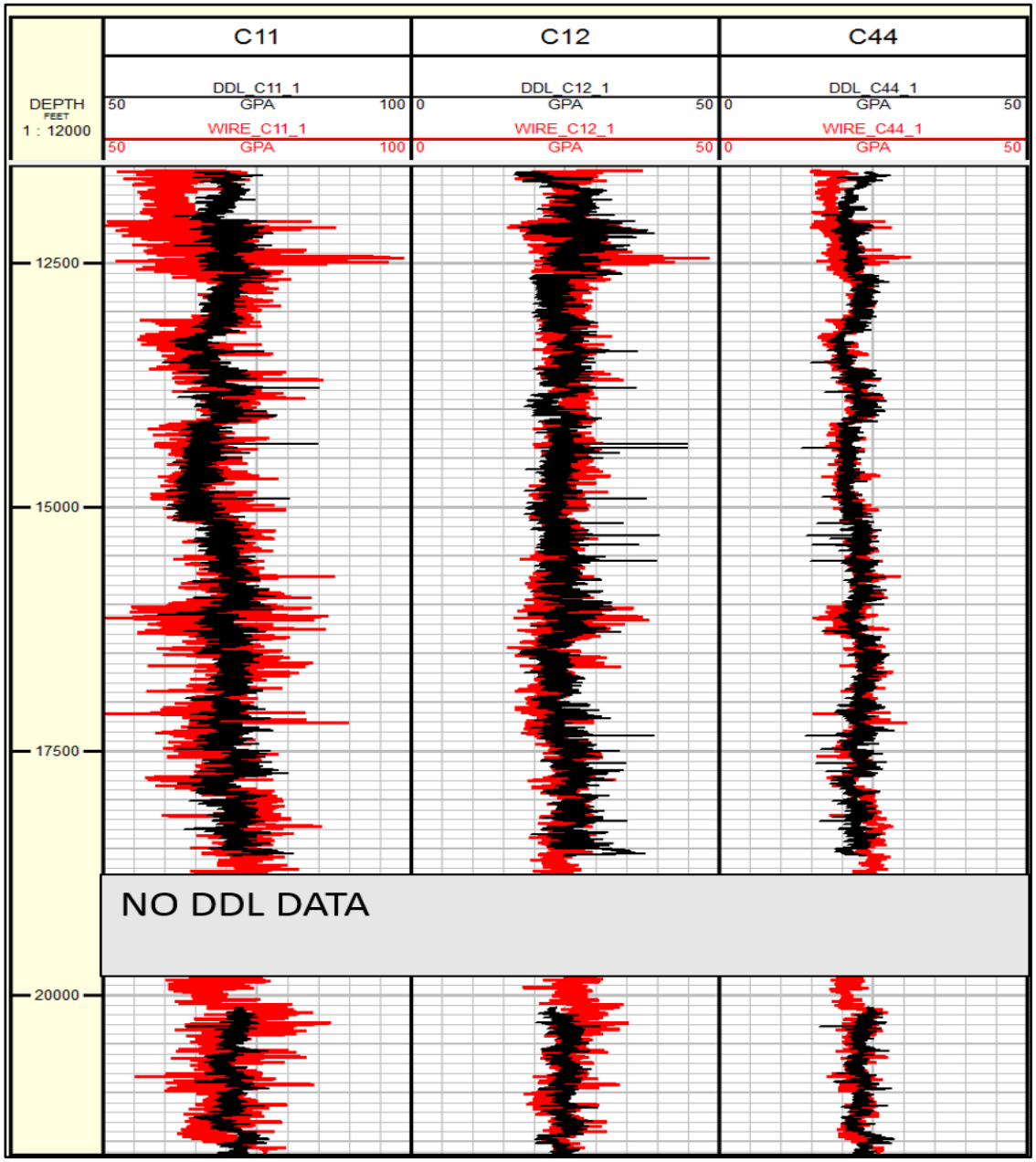

Figure 8. Comparison of the sonic derived tensors vs the DDL tensors plotted on a log. Red is the wireline data while black is the DDL derived data. From left to right, C_{11}, C_{12} and C_{44}

A

Mechanical Properties: Given the good agreement between the stiffness tensors, it is not surprising there is a good agreement between Dipole and DDL Poisson's ratio (PR) and Young's Modulus (YM). As with previous figures red is for dipole and black is for DDL data. (Fig. 9) Once again we see the heel of the well having a different dipole value due to coherency issues. The data presented here is the dynamic values

The dynamic values shown in Fig. 9 match up well with lab derived properties for the Three Forks Formation. Since PR is one of the primary controls on horizontal stress in an isotropic formation, a good match is imperative for fracture modeling (as shown later). Triaxial tests on core plugs from an offset well have shown the TF formation to have an average static PR of 0.26 with a standard deviation of 0.05. Likewise the dynamic YM from ultrasonic core measurements has an average of 7 MPSI or 49GPA. Thus, the lab measurements have a similar average and standard deviation as the DDL and sonic tool. A dynamic to static correction is needed to use YM.

When comparing the DDL and the dipole derived mechanical properties, the average difference between the two PRs is less than 0.03 units which is well within error bars for any measurement including a triaxial load frame. The difference on the YM is less than 6 GPA or ~1 MPSI which is also well within tolerance for laboratory tests. Thus, the error from the DDL calculated properties is similar to the error bars in the lab setting. This close correlation is attributed to properly calculating the constants A-F in matrix B.

Static Vs. Dynamic: A Point of Discussion: It should not be lost that the mean values used to scale the input data were in fact taken from sonic derived measurements of the rock properties, therefore the solution is inherently biased towards a dynamic representation of the media where long-term production and reservoir stimulation are inherently dominated by the static moduli. While it is entirely possible to scale the data to what may be considered static moduli, here the comparison of the relative values of the sonic and drilling induced vibrations is what is desired. It should be noted that understanding the static vs dynamic prospect of the data would involve the identification of systematic variations between the sonic derived rock properties and the rock properties from the DDL data where other petrophysical measurements, such as NMR, would be used to determine fluid properties. This is an on-going area of research.

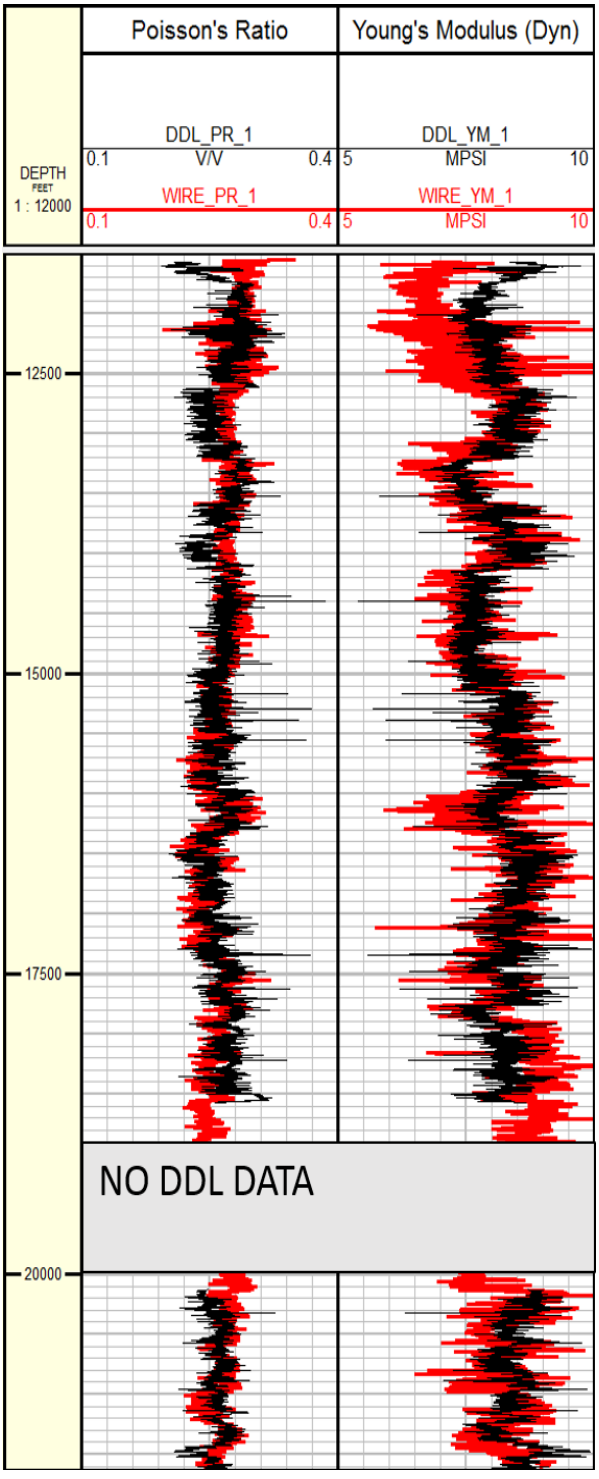

Figure 9. Comparison of the sonic derived mechanical properties vs the DDL tensors plotted on a log. Red is the wireline data while black is the DDL derived data. On the left track is plotted the Poisson's ratio while the right track contains the Young's modulus.

A

Fractures: The fracture flag (FF), again in black, (Fig. 10) from the DDL tool is calculated using changes in VTI and HTI stiffness coefficients (see methods section). The DDL fracture flag, as reported in the data processing section, is a construct based on the VTI and HTI Young's modulus ratio. When the vertical Young's modulus is greater than the horizontal Young's modulus then the cross-over in mechanical heterogeneity would indicate that the rock is more compliant horizontally. We can use this to infer the presence of fractures. The DDL fracture flag (FF) is computed on a probability basis from 0-100% chance.

An image log was run where the fractures were manually observed and counted by an interpreter. Then the number of fractures per 10ft was tabulated as P10. (M. Mauldon & W. Dershowitz, 2000) The count in any given 10ft ranges from 0 to14 fractures present. The interpreter's count of fractures per 10ft is shown in red in Fig. 10.

Comparing these two numbers we see that both metrics tabulated a large number of fractures along the wellbore. (Fig. 10) The fractures appear to be grouped into swarms with the largest number existing near ~15,000 ft md and the toe of the well. The Image log interpreter tabulated 402 continuous fractures of which ~86% were resistive. Meanwhile the DDL fracture flag found 497 features with a greater than 10% probability. If we filter the probabilistic DDL fracture flag to 50% chance or greater and also filter the fracture count from the image logs to >4 fracture per 10ft we find that the data lines up with decent agreement. (blue box on right hand side of fig. 10) Thus with this methodology of tabulating fractures we can conclude that the DDL tool can ascertain the location of fracture swarms. But perhaps not effectively find partial fractures, lone fractures or fractures that are similar in composition to the matrix. This is an ongoing area of research since identifying offset hydraulic fractures without having to run an image log would be highly beneficial.

Because of depth control, the fracture flag from the DDL and the image log do not line up or cross plot very well on a point for point basis. In general, the drilling depth accuracy is unlikely to pin down a one-inch feature precisely. Thus the DDL fracture flag may suggest that fractures are present but the depth could be shifted by a few feet from where the image log pinpoints it.

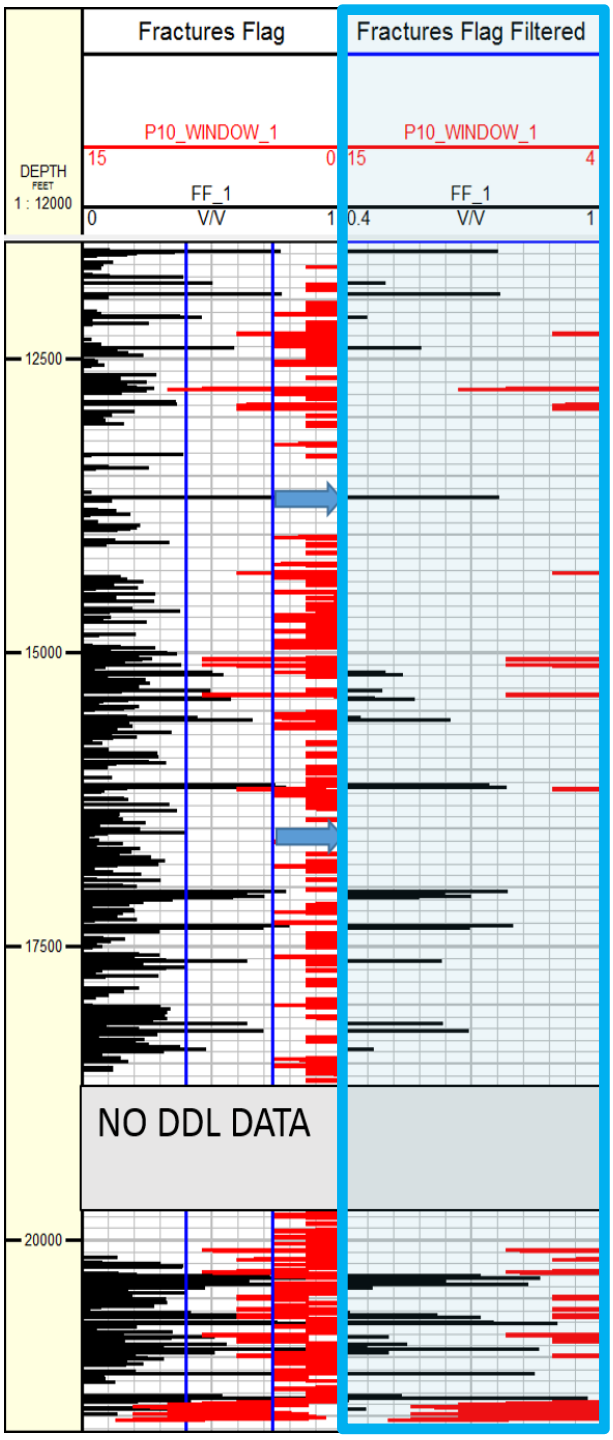

Figure 10. Comparison of the image log counted natural fractures and the fracture flag from the DDL tool. Left track contains all the data while the right track contains just the fracture swarms from the image and fractures with >50% probability from the DDL tool.

Completion Simulation: Once the mechanical properties were acquired using the DDL tool, the natural next step is to try and customize the completion design to optimize efficiency. The current industry trend is to shift geometrically equally spaced stages around so that each stage encounters a roughly homogenous stress field. Therefore we must calculate a minimum horizontal stress. Using equation (2) (Savage, Swolfs and Amadei, 1992) we can calculate the minimum principle stress in an isotropic medium (see appendix A).

$$\sigma_{hmin} = \frac{v}{1-v}(\sigma_{ovb} - \alpha Pp) + \alpha Pp + strain\ terms \quad (2)$$

Where σ_{hmin} is the minimum horizontal stress, v is the Poisson's ratio, α is biot's coefficient, Pp is the pore pressure, σ_{ovb} is the vertical stress from overburden. With the Poisson's Ratio from the DDL and a-priori knowledge of the pore pressure and biot's coefficient we can calculate a minimum horizontal stress. Since we are missing DDL data near the toe of the well, the horizontal dipole Poisson's was substituted over that interval.

After calculating the min horizontal stress the task now is to group stages so that each section is in a homogeneous stress field. In this case we first binned the stress distribution into 100 psi increments and compared qualitatively by color. (Fig. 11 &12) It is now easy to identify areas of low and high stress along the length of the lateral. The red line going down the middle of figure 12 is the average min horizontal stress for the entire lateral. It is likely these changes in stress in the lateral are primarily due to changes in position in the vertical section. In other words they are steering related. You can easily identify the higher stress areas towards the heel and toe of the well and also see areas of low stress near the middle of the well. These areas with sudden shifts in minimum horizontal stress necessitated shifting five of the geometric stages laterally in order to "group like rock with like". (Fig. 13)

Once the min stress was generated, we then imported stress grid into a completion design software (Fig. 13) where we were able to fill in the stress at each grid cell and generate a 3D stress grid. By shifting the five stages into "like rock" we were able to increase modeled efficiency and reduce wasted energy on a per stage basis. This theory of moving stages has been expounded upon by (Jahandideh & Jarfarpour, 2014).

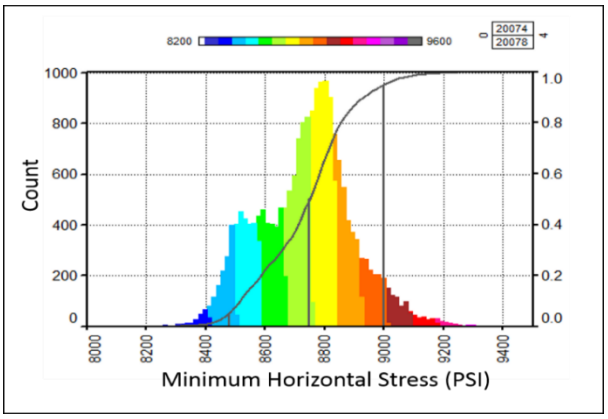

Figure 11. Histogram of the calculated minimum horizontal stress from the DDL tool. Binned with a color bar every 100 psi.

SUMMARY BUT NOT CONCLUSIONS

It is evident from the results that more laboratory measurements on the DDL tool would be beneficial. But in this case, by measuring accelerations while drilling we are able to predict the stiffness tensors in an isotropic medium. We are able to achieve this by taking the axial, centripetal and angular accelerations from a bit sub measured at 1 kHz and via matrix B convert them to tensors C_{11} and C_{12}.

$$\begin{bmatrix} Dd_1 & (Ed_2 + Fd_3) \\ Ed_2 & (Dd_1 + Fd_3) \\ Fd_3 & (Dd_1 + Ed_2) \end{bmatrix} \begin{bmatrix} C_{11} \\ C_{12} \end{bmatrix} = \begin{bmatrix} Aa_1 \\ Ba_2 \\ Ca_3 \end{bmatrix}$$

By solving for the scalars, A-F in a known formation or by using dipole data we can translate the accelerations into tensors and thereby measure the mechanical properties of the formation. We see a good match with error less than < 10% between dipole predicted properties and the DDL predicted mechanical properties. Also fracture swarms were identified using a probabilistic method involving a ratio of HTI and VTI young's and stress.

Once we have obtained the Poisson's ratio and Young's modulus we can generate a calculated minimum horizontal stress and begin doing some hydraulic fracture simulation. In this case, we shifted five stages laterally in order to group them with "like rock". The theory is that grouping the stages in a more homogeneous environment will yield increased energy efficiency and translate to more hydraulically fractured surface area and therefore higher production rates. This DDL technology is continuing to be developed.

A

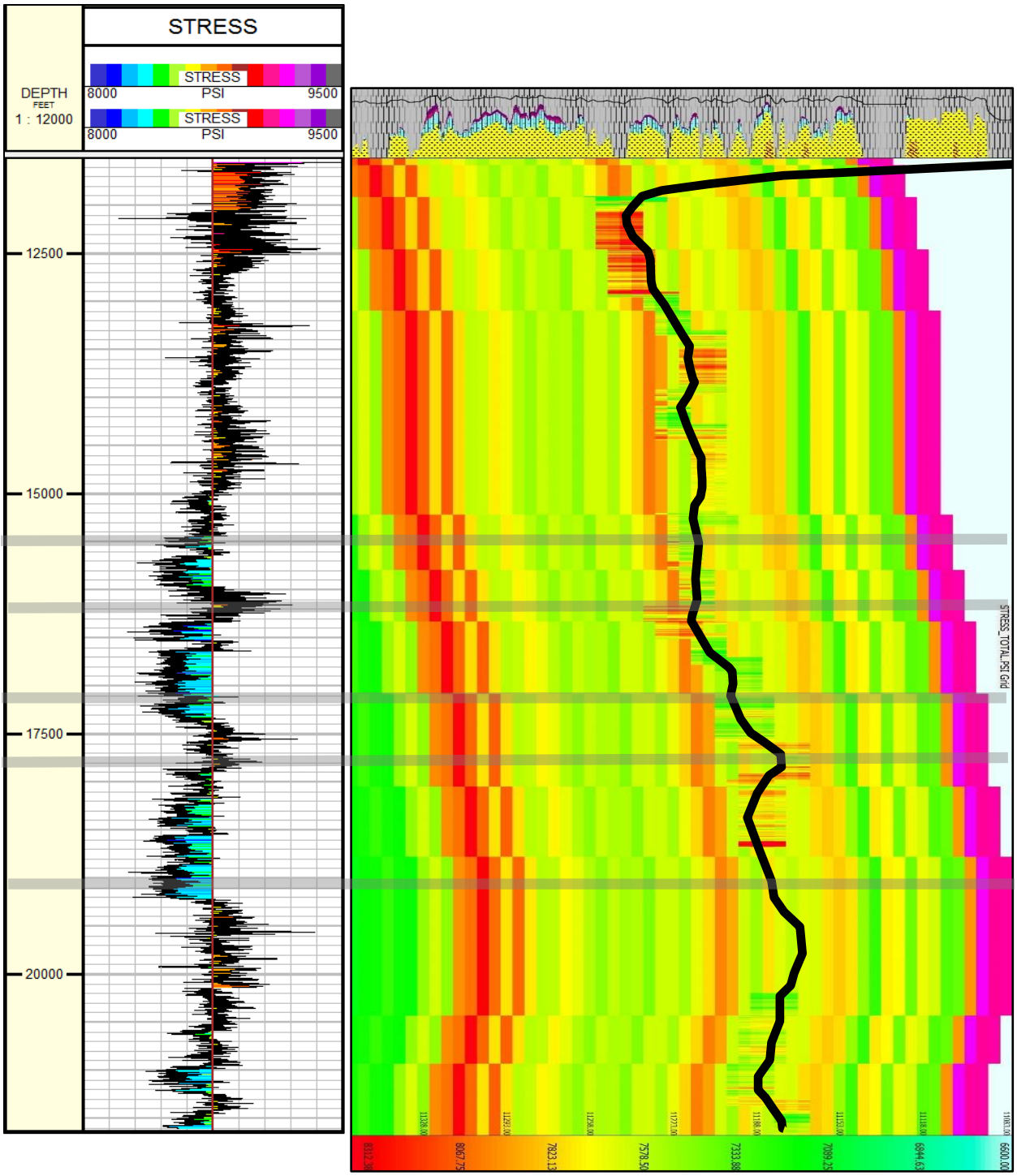

A

Figures 12 (Left). Minimum horizontal stress calculated from the DDL tool and colored based on the histogram data in figure 11.

Figure 13 (Right). Mechanical simulation of the well based on the DDL data. Shifted stages are in grey and cross-cut both figure 12 and 13. Stages were shifted to group “like rock”

REFERENCES

Anna, L.O., Polastro, R., and S.B. Gaswirth, 2013, Williston Basin Province—Stratigraphic and structural framework to a geologic assessment of undiscovered oil and gas resources, chap. 2 of U.S. Geological Survey Williston Basin Province Assessment Team, Assessment of undiscovered oil and gas resources of the Williston Basin Province of North Dakota, Montana, and South Dakota, 2010 (ver. 1.1, November 2013): U.S. Geological SurveyDigital Data Series 69–W, 17 p.

Brune, J. N., 1970. Tectonic Stress and the Spectra of seismic shear waves from earthquakes, Journal of Geophysical Research, vo. 75, no. 26, Sept 10, 1970.

Esmaeili, A., Elahifar, B., Fruhwirth, R. K., and G. Thonhauser, 2013. Formation prediction model based on drill string vibration measurements using laboratory scale rig, SPE/ADC Middle East Drilling Technology Conference and Exhibition, Dubai, UAE, 7-9 October, 2013.

Jahandideh, A., and B. Jafarpour, 2014. Optimization of Hydraulic Fracturing Design under Spatially Variable Shale Fracability. SPE-169521-MS. SPE Western North American and Rocky Mountain Joint Meeting, 17-18 April, Denver, Colorado, 2014.

Karakus, M., T. May and D. Ollerenshaw, 2013. Acoustic emission signatures of rock cutting response of an impregnated diamond drill bit, Proceedings of the World Congress on Engineering, Vol III, WCE 2013, July 3-5, 2013, London, U.K. 2013.

Kumar, B. R., Vardhan, H., and M. Govindaraj, 2011. Prediction of Uniaxial Compressive Strength, Tensile Strength and Porosity of Sedimentary Rocks Using Sound Level Produced During Rotary Drilling, Rock Mechanics and Rock Engineering, September 2011, Volume 44, Issue 5, pp 613–620.

Mauldon M. and W. Dershowitz, 2000, A Multi-Dimensional System of Fracture Abundance Measures, Geological Society of America Annual Meeting, Reno, NV, 2000.

Mavko, G., Mukerji, T., and J. Dvorkin, 2009. The Rock Physics Handbook 2nd Edition. University Printing House, Cambridge CB2 8BS, United Kingdom. pp 21-40.

Murphy, E., S. R. Barraza, M. Gu, M. Far, J. Quirein, 2015. New Models for Acoustic Anisotropic Interpretation in Shale, SPWLA 56th Annual Logging Symposium, July 18-22, 2015.

Murphy, E.C., Nordeng, S.H., Juenker, B.J. and J.W. Hoganson, 2009. North Dakota Stratigraphic Column. North Dakota Geological Survey, Department of Natural Resources. Miscellaneous Series 91, 2009.

Nakken, E. I., Baltzersen, and B. Kristensen, 1990. Characteristics of drill bit generated noise, SPWLA 31st Annual Logging Symposium. June 24-27.

Savage, W.Z., Swolfs, H.S. & B. Amadei. 1992. On the State of Stress in the Near-Surface of the Earth's Crust Pure and Applied Geophysics (1992) 138: 207.

ACKNOWLEDGEMENTS

The Authors would like to thank Fracture ID's Geomechanical Specialist Jesse Havens, Completions Engineer Eric Romberg and Manager of Technology Development Jeff Godwin who have worked tirelessly over the past year to overcome the myriad of unforeseen technical challenges posed by the processing and analysis of drilling induced vibrations to determine stress and strain and obtain in-situ measurements of mechanical rock properties and rock property relationships.

A

APPENDIX A

A Brief Note on Hooke's Law, Stress, Strain & 4th Order Tensors for the Uninitiated

For any given linear elastic material, its' deformation can be described by a stress strain relationship defined by the stiffness. This is an expansion and transformation of Hooke's law for springs.

$$F = -k\,X$$

$$\sigma = E * \varepsilon$$

$$\sigma_{ij} = C_{\alpha\beta}\,\varepsilon_{kl}$$

Above is Hooke's Law, where F is force, k is the spring constant and X is displacement. If you consider the plane the force is acting upon, you can transform Hooke's Law into stress (σ) and strain (ε) with the young's modulus or stiffness (E) as the relationship between the two. If we consider that any given rock has three principal stresses and strains which include shear stresses/strains and if we rotate into the principal stress direction, we can then write our transformed Hooke's law as a matrix where stress is equal to its' nine components. Note that by convention, with the below figure, the x direction is denoted by subscript 1, y direction is subscript 2 and z direction is subscript 3. Also by convention, compressional stresses are written with σ and shear stresses are written with τ.

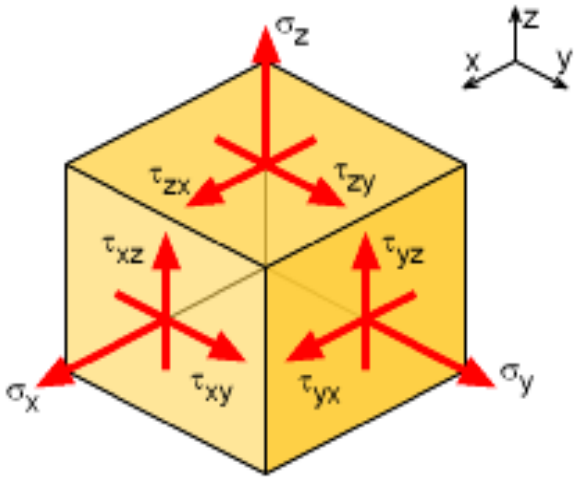

$$\sigma_{xyz} = \begin{bmatrix} \sigma_{xx} & \tau_{xy} & \tau_{xz} \\ \tau_{yx} & \sigma_{yy} & \tau_{yz} \\ \tau_{zx} & \tau_{zy} & \sigma_{zz} \end{bmatrix}$$

$$\sigma_{ij} = \begin{bmatrix} \sigma_{11} & \tau_{12} & \tau_{13} \\ \tau_{21} & \sigma_{22} & \tau_{23} \\ \tau_{31} & \tau_{32} & \sigma_{33} \end{bmatrix}$$

Given that the rock is not spinning, the forces are symmetrical and we can eliminate three of the shear stresses. Therefore we are left with three compressional stresses and three shear stresses which in turn each generate a strain.

$$\sigma_{ij} = \begin{bmatrix} \sigma_{11} & \tau_{12} & \tau_{13} \\ & \sigma_{22} & \tau_{23} \\ SYM & & \sigma_{33} \end{bmatrix}$$

We can now return to the stress strain relationship in that we started with where stress (σ or τ) and strain (ε) are related by the stiffness of the material.

$$\sigma_{ij} = C_{\alpha\beta}\,\varepsilon_{kl}$$

$$\begin{bmatrix} \sigma_{11} \\ \sigma_{22} \\ \sigma_{33} \\ \tau_{12} \\ \tau_{13} \\ \tau_{23} \end{bmatrix} = C_{\alpha\beta} \begin{bmatrix} \varepsilon_{11} \\ \varepsilon_{22} \\ \varepsilon_{33} \\ \varepsilon_{12} \\ \varepsilon_{13} \\ \varepsilon_{23} \end{bmatrix}$$

Since we have six stresses and six strains, we can expand the stiffness term to thirty-six 4th order tensors (C_{ijkl}). We use Voigt's notation to reduce that to just two numbers in each subscript ($C_{\alpha\beta}$) because people don't like writing four numbers repeatedly. Luckily thanks to symmetry again, there are not really thirty-six independent tensors. Because of the unique strain energy potential $C_{ijk} = C_{kijl.}$, this reduces the number of variables to twenty-one which would be tri-clinic system. Now if we assume symmetry between the different sides of the cube the number of unique 4th order tensors drops rapidly. In a monoclinic system there are thirteen unique tensors. For an orthorhombic system there are nine. In a vertically transverse isotropic (VTI) where the one axis is unique but the other two are equal there are five independent tensors. Finally, in an isotropic system where the medium is homogeneous and has maximum symmetry there are only two independent tensors to worry about.

Isotropic stiffness matrix:

$$C_{\alpha\beta} = \begin{bmatrix} C_{11} & C_{12} & C_{12} & 0 & 0 & 0 \\ C_{12} & C_{11} & C_{12} & 0 & 0 & 0 \\ C_{12} & C_{12} & C_{11} & 0 & 0 & 0 \\ 0 & 0 & 0 & C_{44} & 0 & 0 \\ 0 & 0 & 0 & 0 & C_{44} & 0 \\ 0 & 0 & 0 & 0 & 0 & C_{44} \end{bmatrix}$$

Thus, in an isotropic system we have three 4th order tensors that fully describe the elasticity of the material. Where the stiffness in any of the principal directions is equal and homogeneous. Essentially if you measure the stiffness of this material it doesn't matter which direction you take the measurement, you will get the same number every time. You might be thinking "But you just said we only need two unique values in an isotropic case." There is an additional simplification in most of these matrices for C_{12} where we can calculate it from the other tensors. With the below relation we can reduce the three unknowns to just two unique tensors that describe the elasticity, C_{11} and C_{44}.

$$C_{12} = C_{11} - 2C_{44}$$

C_{11} and C_{44} can be calculated from log measured values as denoted in equations below. Where VP is the compressional velocity, VS is the shear velocity and ρ is the bulk density of the material.

$$C_{11} = \rho VP^2$$

$$C_{44} = \rho VS^2$$

Vertically Transverse Isotropic stiffness matrix:

When the matrix is vertically transverse isotropic (VTI), as is often the case with shales or other laminar bedding, we use a different matrix and equations to determine the stiffness tensors. In a VTI medium the stiffness in the z direction has a unique value while the stiffness in the x and y dimension are equal. Ergo, now the directionality of measuring the stiffness is important. If you measure the horizontal stiffness you will get a different answer than if you measure the vertical stiffness. Note that VTI and HTI are essentially identical just rotated versions of one another. If you rotate a VTI rock 90 degrees on one of the horizontal axes it becomes HTI. HTI rocks are typically rocks with vertical laminated bedding or fractures. For the below equations for VTI tensors, by convention 0° degrees is perpendicular to the laminar features and 90° degrees is parallel to the laminar features, while 45° degrees is diagonal to both. The subscript VTI is to denote the difference between the two matrixes. It is still a $C_{\alpha\beta}$ matrix

$$C_{\text{VTI}} = \begin{bmatrix} c_{11} & c_{12} & c_{13} & 0 & 0 & 0 \\ c_{12} & c_{11} & c_{13} & 0 & 0 & 0 \\ c_{13} & c_{13} & c_{33} & 0 & 0 & 0 \\ 0 & 0 & 0 & c_{44} & 0 & 0 \\ 0 & 0 & 0 & 0 & c_{44} & 0 \\ 0 & 0 & 0 & 0 & 0 & c_{66} \end{bmatrix}$$

$$C_{33} = \rho V_p^2(0°)$$

$$C_{11} = \rho V_p^2(90°)$$

$$C_{44} = \rho V_s^2(0°)$$

$$C_{66} = \rho V_s^2(90°)$$

$$\boldsymbol{C_{13}} = \sqrt{\frac{\left(4\rho V_p^2(45°) - C_{11} - C_{33} - 2C_{44}\right)^2 - (C_{33} - C_{44})^4}{4}} - C_{44}$$

Note that in the VTI matrix, the previous simplification for C_{12} no longer applies. While similar, it is important to use the horizontal shear tensor instead of the vertical one.

$$C_{12} = C_{11} - 2C_{66}$$

You may now notice that we are under constrained. A simple dipole sonic will not resolve five unknowns with just two measurements and a density. Thus it is necessary to have either a-priori information or make assumptions about different properties as in Murphy, et. al. 2015. The C_{13} tensor is especially elusive when making downhole measurements. For more information on this subject please consult Gary Mavko's book The Handbook of Rock Physics 2nd ed. (2009) Perhaps with further laboratory work the DDL tool can provide the missing link to get all the needed tensors to satisfy the VTI matrix.

A

ABOUT THE AUTHORS

Adam Haecker is a Senior Petrophysicist in the new ventures group of a major independent oil company in Oklahoma City, OK. He is currently researching a diverse range of topics including earth stress prediction with an emphasis on mechanical anisotropy, mineralogy in organic shales, pore pressure prediction in organic shales and permeability measurements in unconventional reservoirs including klinkenberg corrections. He obtained his B.S. in geology from Texas A&M University in 2007. He joined his current company in 2014 and has been in the E&P industry for ten years. Previously with Chesapeake Energy, Cabot Oil and Gas and Weatherford Wireline. He is the President of the Oklahoma City chapter of the SPWLA. His hobbies include model building and learning Japanese.頑張って!

Eric Marshall is Manager of Completions Technology for Fracture ID where he is undertaking an industry leading role using in-situ measurements rock properties and rock property relationships for compiling user friendly, completions ready formats to assist operators with maximizing the value of their completions. Eric is highly regarded in coiled tubing and hydraulic fracturing operations and successfully managed Haliburton's, turn of the century, global expansion of their Pinpoint Stimulation technology. Later, during his 9 years with IPT, he practiced reservoir engineering and completions design, specializing in the economic optimization of field developments. Eric has been a member of SPE for 14 years and is a registered professional (petroleum) engineer in the states of Colorado, Texas, Oklahoma, North Dakota, Wyoming and Ohio. He received his B.S. degree in Mechanical Engineering from the Colorado School of Mines in December of 2002.

James D Lakings is Chief Technology Officer for Fracture ID where he is leading the early and ongoing scientific investigations involving the processing and analysis of near-bit drilling induced vibrations to obtain mechanical rock property and rock property relationships. He has coined this new geophysical field Drillbit Geomechanics. He has enjoyed nearly 20 years' worth of industry experience working previously with Anadarko Petroleum, Microseismic Inc, Earthwater Global and Geovesi Services. Dr. Lakings has a B.S. in Geophysics from The New Mexico Institute of Mining and Technology in 1992 and received his PhD in Arts and Sciences from Duke University in 1997.

Josh Ulla is VP Business Development for Fracture ID where he is charged with finding innovative, new solutions to industry leading problems in the exploration and exploitation of unconventional reservoirs through the application and use Fracture ID's award winning Drillbit Geomechanics Technology. Josh started working for ExxonMobil in Houston, Texas in the Geophysical Operations and Formation Evaluations Groups where he was recognized as the Global Borehole Seismic Expert, and was relied upon to model, design, acquire, process, and interpret seismic and petrophysical data. He has research interests in unconventional geophysical data analytics. Originally from Canada, Josh holds a B.S. in Mathematics and an MS Geophysics from Carlton University.

A